

A new methodology for studying the spreading process of mining subsidence in rock mass and alluvial soil: an example from the Huainan coal mine, China

Dawei Zhou^{1,2} · Kan Wu¹ · Liang Li¹ · Xinpeng Diao¹ · Xianshen Kong¹

Received: 16 December 2015 / Accepted: 30 March 2016 / Published online: 6 April 2016
© Springer-Verlag Berlin Heidelberg 2016

Abstract Alluvial soil plays an important role in ground subsidence caused by coal mining and groundwater extraction. Coal mining areas covered with thick alluvial soil (CMATASs) are widely distributed in China, and ground subsidence in these areas exhibits unique features—for instance, the maximum subsidence is greater than the extracted coal seam thickness. Consequently, studies on the regularity and mechanism of mining subsidence in CMATASs have gained much attention. However, current research methods mainly involve numerical/physical simulation and theoretical analysis, while convincing verification using field data is lacking, leading to limited research results and weak practicability. This paper proposes a new approach for studying the spreading process of mining subsidence in rock mass and alluvial soil, as well as the response of alluvial soil to mining subsidence in these areas, through the use of field data. This approach includes the following steps and assumptions: First, the overlying rock mass and alluvial soil are regarded as a dual medium; subsidence data obtained in coal mining areas covered with thin (non-)alluvial soil (N-CMATASs) are taken as the bedrock surface subsidence in the CMATASs (the lower boundary condition of thick alluvial soil). Second, ground subsidence data obtained in CMATASs are taken as the

upper boundary condition of the thick alluvial soil. And lastly, by considering the measured mining-induced overburden fracture datum and geo-mining conditions in CMATASs, we can study the spreading process of mining subsidence in rocks and soils and determine the underlying mechanism as well as the response of the soil to mining subsidence in CMATASs. A major feature of the proposed approach is that the overlying rock mass and alluvial soil can be separated and the measurement data can be obtained in different boundaries, thus compensating for the shortage of measured data in current study methods. This approach was successfully applied in the Huainan coal mining area in China, and can provide a basis for accurate calculation of ground subsidence in similar mining areas.

Keywords Thick alluvial soil · Overlying strata · Mining subsidence · Borehole logs · Probability integral model

Introduction

Alluvial soil plays an important role in the process of ground subsidence caused by coal mining (He et al. 1991; Huayang et al. 2010; Kratzsch 1983; Peng and Zhang 2007; Peng 1992; Ronning et al. 1995; Tan et al. 2002; Wang et al. 1997; Yuan et al. 2001; Zhang et al. 1999, 2002; Zhou 2014; Zhou et al. 2015) as well as groundwater extraction (Caro Cuenca et al. 2013; Chai et al. 2004; Li and Yu 1997; Ortega-Guerrero et al. 1999; Phien-vej et al. 2006; Xu et al. 2007; Xue et al. 2005). In China, coal mining areas with quaternary alluvial soil layers less than 50 m, more than 100 m, and more than 300 m thick are called thin (the usual geological condition), thick, and mega-thick alluvial mining areas, respectively (He et al. 1991; Industry SBoC 2004; Liu et al. 2012; Zhou 2014;

✉ Kan Wu
dwzhou2008@126.com; wukan6899@263.net

¹ School of Environment Science and Spatial Informatics, China University of Mining and Technology, Xuzhou 221116, China

² State Key Laboratory for Geomechanics and Deep Underground Engineering, China University of Mining and Technology, Xuzhou 221116, China

Zhou et al. 2015). In studies of ground subsidence caused by underground mining, current field measurement protocols and research methods are quite capable of providing accurate results in usual geological conditions. Some of these results have been used in production (Alejano et al. 1999; Baochen and Ronggui 1981; Brady and Brown 2004; Cui et al. 2000; Djameluddin et al. 2011; Donnelly et al. 2001; Guéguen et al. 2009; He et al. 1991; Holla 1997; Kratzsch 1983; Li et al. 2010, 2014; Marschalko et al. 2011; Nicieza et al. 2005; Oconnor and Dowding 1992; Peng and Zhang 2007; Qian et al. 2003; Sheorey et al. 2000; Singh and Yadav 1995; Wu et al. 2000, 2012a, b, 2013, 2014). In coal mining areas covered with thick alluvial soil, however, mining subsidence exhibits certain unique phenomena. For example, the subsidence factor is greater than 1.0, i.e., the maximum subsidence is greater than the extracted coal seam thickness, and the scope of ground subsidence is much wider, and the horizontal displacement is greater than the vertical subsidence at the trough border. In addition, the active period of ground movement is more intense and concentrated, and the duration of ground movement is longer (Ge and Yu 2006; Sui 1992; Sui and Di 1999; Tan et al. 2002; Wang et al. 1997; Wu et al. 1998, 1999, 2002; Yang et al. 1994; Yuan and Wu 2003; Yuan et al. 2001).

Coal mining areas covered with thick alluvial soil (CMATASs) are widely distributed in China, concentrated mainly in mining areas of Huaibei, Huainan, Yanzhou, Datun, Jiaozuo, Pingdingshan, Yongxia, Kailuan, and Xingtai, as well as mining areas in East China, Central China, North China, and Northeast China (He et al. 1991; Industry SBoC 2004; Liu et al. 2012; Sui 1992; Yuan and Wu 2003; Zhou 2014, 2015). Various research methods have been employed to date for the study of ground subsidence in CMATASs. For example, Wu et al. (1999, 2002) adopted a physical simulation method to study the mode of transfer and transfer range of mining subsidence in the soil mass. Sui (1992; Sui and Di 1999) and Di (Sui 1992; Sui and Di 1999) used a centrifugal model test and finite element method (FEM) to analyze the particularities of subsidence caused by soil consolidation and secondary consolidation from an engineering geology perspective. Zhang et al. (1999) deduced a movement equation of the bedrock surface based on the principle of elastic–plastic deformation. Liu et al. (2012) obtained differences between bedrock and surface basin movement using a physical simulation method. In addition, some scholars (Alejano et al. 1999; Cundall 1990; Gao and Yu 2007; Huayang et al. 2010; Kidybinski and Babcock 1973; Lu and Wang 2015; Oconnor and Dowding 1992; Ren et al. 2010; Wu et al. 2002; Yasitli and Unver 2005) have employed numerical simulations including the distinct element method (DEM), FEM, and similar-material simulation (i.e.,

physical simulation) to investigate ground movement and deformation in CMATASs.

There is general consensus that mining subsidence in CMATASs is affected by the overlying rock mass, the alluvial soil, and the interaction between rocks and soils (He et al. 1991; Huayang et al. 2010; Liu et al. 2012; Wang et al. 1997; Zhang et al. 1999; Zhou 2014; Zhou et al. 2015). Thus it is appropriate to consider the entire overlying strata as a dual medium: rock mass and alluvial soil. However, observational data inside rock mass and soil is sparse. The methods currently in use largely involve physical/numerical simulation and theoretical analysis, and each has shortcomings and limitations, leading to weak practicality of the research results.

In view of these problems, and in order to make full use of measured data, in this study we have proposed a new methodology: first, regarding the overlying rock and alluvium as a dual medium and separating the processes of mining subsidence spreading in rocks and soils, and then conducting comprehensive research on the influence of the rocks and soils on mining subsidence. With the adoption of the new methodology, we can study the mechanism of mining subsidence in CMATASs in detail and provide a basis from which to fully explain the particularities of the subsidence and obtain an accurate estimation of ground subsidence that occurs in CMATASs.

The new methodology and its implementation

The methodology

As mentioned above, because of the inherent difficulties of observation inside rock mass and soil, little observational data have been obtained. The monitoring of ground surface subsidence, on the other hand, is more convenient, and there is a vast amount of field measurement data on ground subsidence in China. Therefore, this data can be used as a substitute for subsidence inside the rock mass when certain conditions are fulfilled, as described below.

According to coal mining subsidence theory, for any two mining areas, if the lithology of the overlying rock, stratum structure, and geo-mining conditions such as the height/width of the mining seam, seam inclination, mining methods, and roof control methods are the same or similar, the ground subsidence between the two should be identical/similar. Furthermore, we can conveniently obtain accurate geo-mining conditions from the coal mining company, making it easy to ensure that the geo-mining conditions are the same or similar between CMATAS and N-CMATAS. However, it is difficult to judge the similarity of the lithology of the overlying rock and stratum structure. In this study, therefore, we put forward a method for

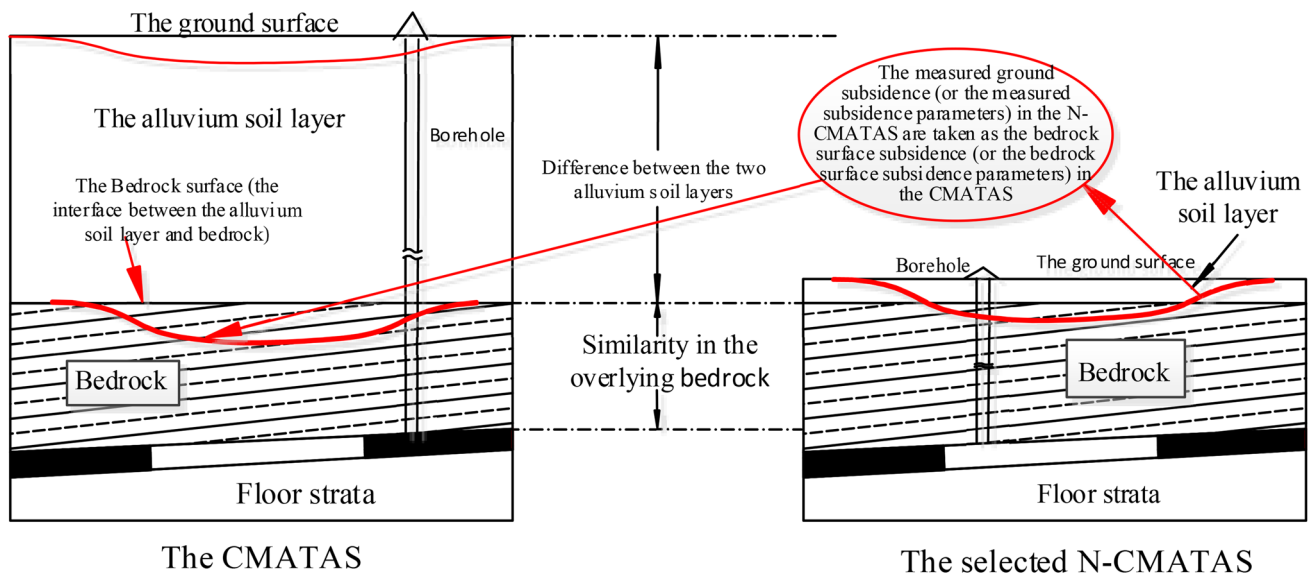


Fig. 1 Generalized model of the new methodology

determining the lithological similarity between two coal mining areas.

Based on the premise that the geo-mining conditions are the same or similar when the lithology of the overlying rocks of CMATAS—the overlying rock is referred to as the bedrock part after removal of the alluvial soil above—and N-CMATAS are assumed to be the same or similar, we can use the measured ground subsidence in CMATAS to substitute the bedrock surface subsidence (the bottom of thick alluvium or the interface between the alluvium and bedrock as shown in Fig. 1) in N-CMATAS. Alluvium thickness is large in relation to mining depth, and it may affect the field stress and thus the caving behavior of strata. Based our research (Zhou 2014), however, the subsidence error caused by differences in field stress between CMATAS and N-CMATAS is within an acceptable range.

The new concept explained in detail

Figure 1 illustrates a generalized model of this novel method based on the abovementioned concept. The details are explained as follows. After a comprehensive determination of the geological and mining factors and the overlying rock mass structure (referring mainly to borehole logs of rock structure after removing alluvial soil) of the CMATAS, we can select an N-CMATAS with similar characteristics. We verify that the height/width of the mining seam, seam inclination, mining method, and the method of roof control are similar between CMATAS and N-CMATAS. We then take the measured ground subsidence (or the measured subsidence parameters) of the selected N-CMATAS as the bedrock surface subsidence in the CMATAS (the lower boundary condition of the thick

alluvial soil), and take the observed ground subsidence data in the CMATAS as the upper boundary condition of the thick alluvium. Considering the measured mining-induced overburden fracture datum and geo-mining conditions during underground mining in the CMATAS, we can separate the entire overlying rock–soil mass into rock mass and alluvium in the CMATAS. Simultaneously, we can obtain measured data of different boundaries. Finally, we can implement a more detailed and accurate study of the process of mining subsidence spreading in rock mass and alluvium and can determine the underlying mechanism and the response of the soil to mining subsidence in the CMATAS.

The implementation steps are presented in detail in the following section, “Detailed steps of implementation.”

Detailed steps of implementation

Step 1 First we must acquire or gather geological and mining factors of the CMATAS, including alluvial layer thickness, thickness of the bedrock (removing the alluvial part), coal mining method, roof control method, coal seam thickness, dip angle of coal seam, and borehole logs of the rock structure obtained by drilling boreholes from the ground down to the rock strata. These provide essential data for selecting the most similar N-CMATAS from alternative N-CMATASs and for a follow-up study. A ground movement observation station (GMOS; He et al. 1991; Tan et al. 2002) should be established on the ground surface of the CMATAS to obtain ground subsidence data, which are taken as the upper boundary condition of the thick alluvium

- Step 2 Based on the acquired geological and mining factors and the overlying rock structure in step 1, we determine an N-CMATAS with similar characteristics. This selection method is described in the section “[Method of determining the similarity in the overlying rock structures between CMATAS and N-CMATAS](#)”
- Step 3 We establish the GMOS in the selected N-CMATAS and monitor the ground subsidence data (or measured subsidence parameters). In this manner, we acquire the lower boundary conditions of the thick alluvial layer
- Step 4 Based on the upper and lower boundary conditions of the thick alluvium in the CMATAS, the response of the soil to mining subsidence in the CMATAS can be determined through further analysis and calculation, and the results elucidate the particularities of mining subsidence in the CMATAS in detail and provide a basis for establishing a prediction model

The implementation of the specific steps is shown in Fig. 2.

Method of determining the similarity in the overlying rock structures between CMATAS and N-CMATAS

We adopt an analogy of borehole logs from the ground down to the rock strata for judging the similarity in the overlying rock structures between N-CMATASs and CMATAS. First, we take a borehole log (remove the alluvial part) of the overlying rock mass in the CMATAS as a standard sample and take the borehole logs of the N-CMATASs as samples to be identified. We then digitize these samples (borehole logs) and extract the lithology eigenvalues from the digitized samples. Based on the lithology eigenvalues of the standard samples and the samples to be identified, we select a coal mining area with thin (non-)alluvial soil (N-CMATAS) with characteristics similar to the CMATAS, taking into account the geomining conditions and rock mass structure. A number of thin (non-)alluvial mining areas can be collected as samples for comparison to the standard samples, and the N-CMATAS with the highest similarity to the CMATAS can be selected. Suitable samples can be identified through the following three steps:

Step 1: Digitization and eigenvalue extraction of borehole logs

Assume that there are m layers of different strata in the overlying rock structure shown in the borehole log. The coal seam in the borehole log is regarded as the origin point, the m layers of different strata are divided into n sections, the thickness of each layer is S_j ($j = 1, 2, \dots, m$), and the

lithology eigenvalue of each section is calculated using the lithology comprehensive evaluation coefficient method (P coefficient method; He et al. 1991; Wu et al. 1998; Yuan and Wu 2003; Zhou 2014). The equation is as follows:

$$p_i = \frac{\sum M_{ij}Q_j}{\sum M_{ij}}, \quad (1)$$

where P_i ($i = 1, 2, \dots, n$) is the lithology comprehensive evaluation coefficient of the i th section, M_{ij} is the normal thickness of the j th layer of the strata in the i th section, and $\sum M_{ij} = S_i$, Q_j is the lithology evaluation coefficient of the j th layer of strata, which can be set according to Table 1.

Step 2: Evaluation of membership degree in the overlying strata structure

Assume that the lithology eigenvalue of each section of standard samples is $P_{k1}, P_{k2}, \dots, P_{kn}$ ($k = 1, 2, \dots, r$), and that there are r samples (number of alternative samples) to be identified. The lithology eigenvalues of the samples to be identified are $P_{k1}, P_{k2}, \dots, P_{kn}$, and the lithology membership degree (marked as u_i) of each section strata is then calculated as follows:

$$u_i = 1.0 - \frac{|P_i - P_{ki}|}{\text{MAX}(P_i, P_{ki})}, \quad (i = 1, 2, \dots, n), \quad (2)$$

where, $\text{MAX}(P_i, P_{ki})$ is the maximum value between P_i and P_{ki} . For example, if $P_i > P_{ki}$, then $\text{MAX}(P_i, P_{ki}) = P_i$.

Step 3: Evaluation of similarity in the overlying strata structure

General similarity between the standard sample and the samples to be identified is calculated using the following equation:

$$C_k = \frac{\sum u_i}{n}, \quad (k = 1, 2, \dots, r), \quad (3)$$

where C_k is the general similarity between the standard sample and the k th samples to be identified. Here, $0 \leq C_k \leq 1$, and the higher the C value, the greater the similarity; similarity will be highest when $C = 1$ and lowest when $C = 0$.

Case study of the CMATAS of the Xieqiao mine in the Huainan coal mining area

General situation

Huainan coal mining area

The Huainan mining area in China is divided into the south (hereinafter referred to as “south area”) and north (hereinafter referred to as “north area”) mining areas by the Huai River, a major river in China located midway between the Yellow and Yangtze rivers (He et al. 1991;

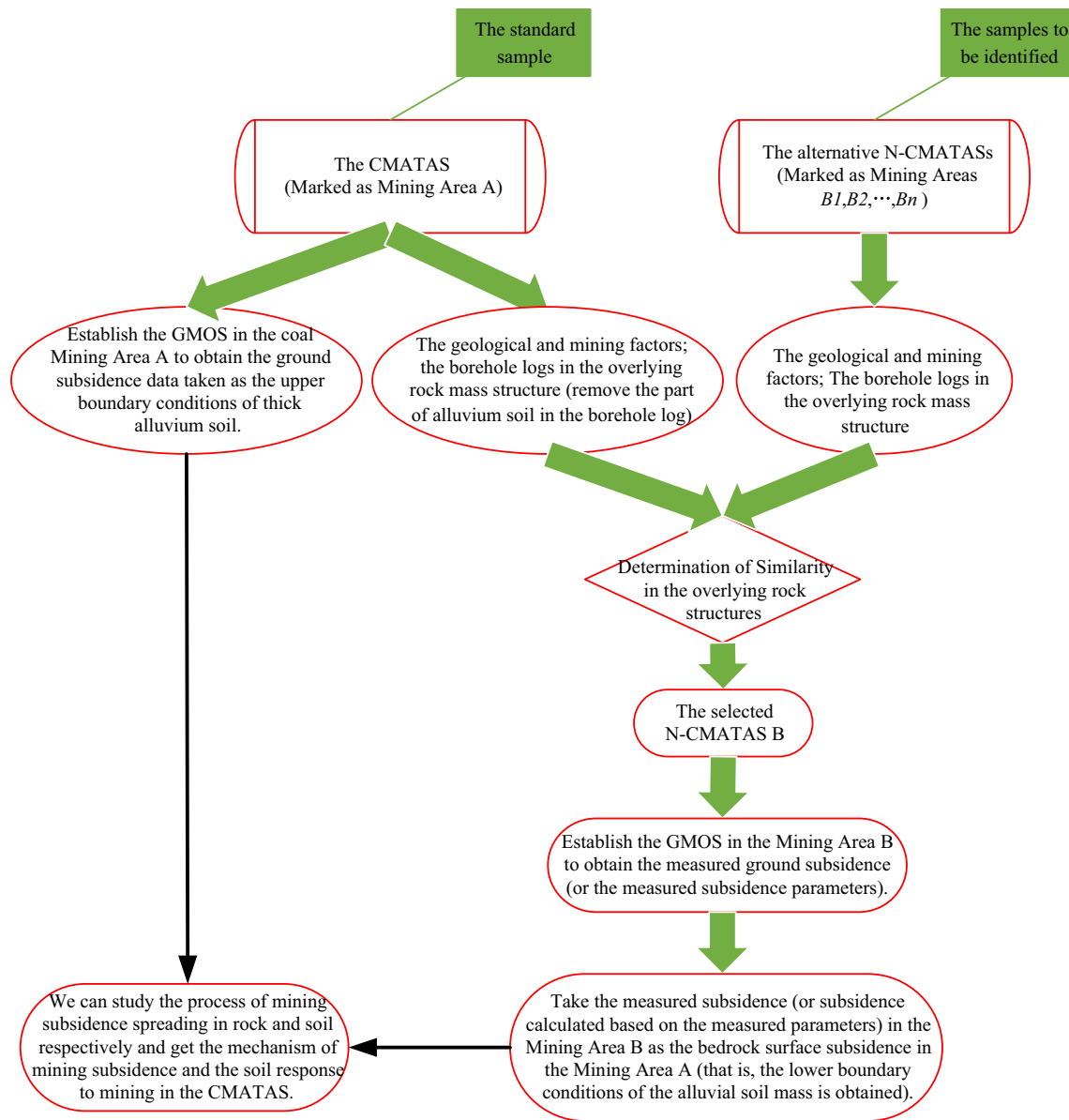


Fig. 2 Detailed steps for implementing the proposed method

Table 1 Lithology evaluation coefficients for reference

Lithology	Strata name	<i>Q</i>
Hard	Hard limestone, hard sandstone, hard marble, non-hard granite	0.0
	Relatively hard limestone, sandstone, marble	0.05
Medium-hard	Ordinary sandstone, iron ore	0.1
	Sandy shale, flake sandstone	0.2
	Hard clay schist, non-hard sandstone and limestone, soft conglomerate	0.4
	All kinds of shales (non-hard), dense marl	0.6
Soft	Soft shale, soft limestone, anthracite, ordinary marl	0.8
	Broken shale, bituminous coal, clay (dense)	0.9
	Soft sandy clay, loess, soft gravel, loose sand layer	1.0

Wu et al. 1998; Yuan and Wu 2003; Zhou 2014). The distribution of the Huainan coal mine is shown in Fig. 3. The north area is a CMATAS, where alluvial thickness is 160–500 m, and the south area is an N-CMATAS, with alluvial thickness of only 20–40 m. Thus the Huainan coal mining area exhibits mining subsidence characteristics of both the N-CMATAS and the CMATAS.

CMATAS of the Xieqiao mine and its GMOS

The Xieqiao mine is located in the north area of the Huainan mining area. The average thickness of coal seams in working face A is 3 m, and the average dip angle is 15°. It features a fully mechanized coal mining technology and longwall full caving for roof control. Mining speed is 34 m per month on average. The actual horizontal length along the strike of working face A is 620 m, and the horizontal length along the dip is 171.8 m. The mining depth is about 550 m, with an alluvial thickness and bedrock thickness of about 400 and 150 m, respectively. The overlying strata structure and lithology are shown in the borehole log in Fig. 5. Mining in working face A started in January 1996 and was finished on June 20, 1997, lasting 18 months.

By the end of December 1995, a ground movement observation station comprising 145 points was established on the ground surface above the aforementioned working face. Strike and dip observation lines were set, as shown in Fig. 4. The first comprehensive field measurement was made in early 1996, and the last was made in March 1998. In total, four comprehensive field measurements (levelling and plane coordinates) and 18 levelling measurements were conducted. The curves (1) of Figs. 12 and 13 show field-measured subsidence profiles along the strike and dip between the first and last measurements, respectively.

Determination of similarity in the overlying rock structures between the Xieqiao mine and the alternative N-CMATASs

Using the proposed research concept and implementation steps, we take the geological and mining conditions of working face A of the Xieqiao mine as a standard sample. The stratigraphic structure or the overlying rock structure refers to the borehole log shown in Fig. 5. In addition, we provide five different working faces from different N-CMATASs (alternative N-CMATASs) as samples to be identified [i.e., $r = 5$; $k = 1, 2, 3, 4, 5$ in Eqs. (2) and (3)]. The corresponding strata structures and detailed geo-mining conditions are shown in Figs. 6, 7, 8, 9, and 10, and in Table 2, respectively.

Each borehole log (including the standard sample and the alternative samples) demonstrating the overlying rock structure or stratigraphic structure is evenly divided into 50 sections [$n = 50$ in Eq. (2)], as shown in Figs. 5, 6, 7, 8, 9, and 10.

According to Eq. (1), we digitized each borehole log, and the lithology eigenvalue of each section was calculated as shown in Figs. 6, 7, 8, 9, and 10. We calculated the membership degree of each section, which is shown in Figs. 6, 7, 8, 9, and 10, using Eq. (2). We then calculated the general similarity between each of the alternative samples (five different working faces of different coal mining areas) and the standard sample (i.e., the Xieqiao mine of the Huainan coal mining area), which is shown in Table 3, using Eq. (3).

As shown in Table 3, among the five alternative samples, the Xinzhuangzi mine in the south area of the Huainan coal mining area had the highest similarity to the standard samples, and the Xieqiao mine in the north area of

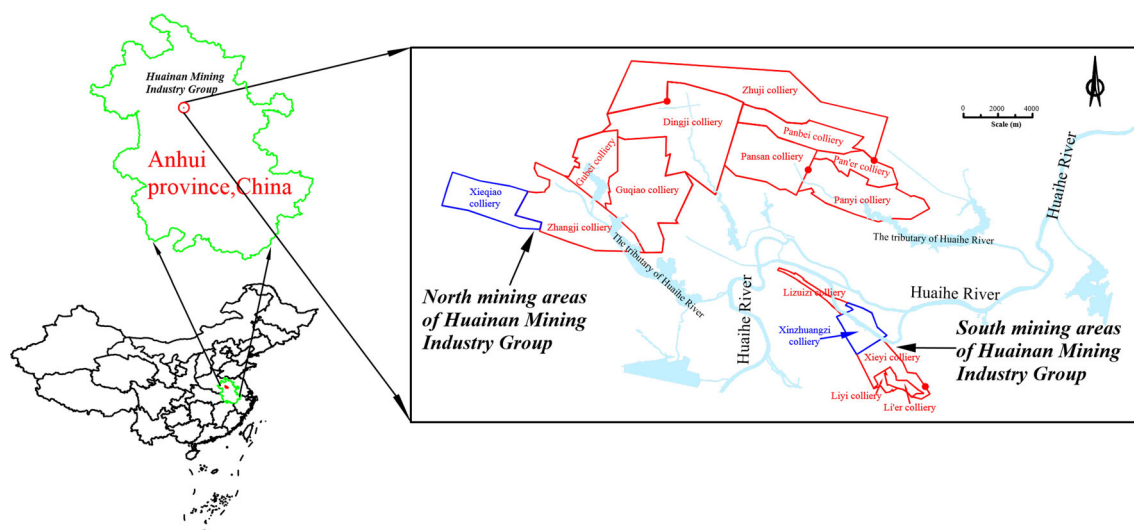


Fig. 3 Distribution of north area and south area of the Huainan coal mining area

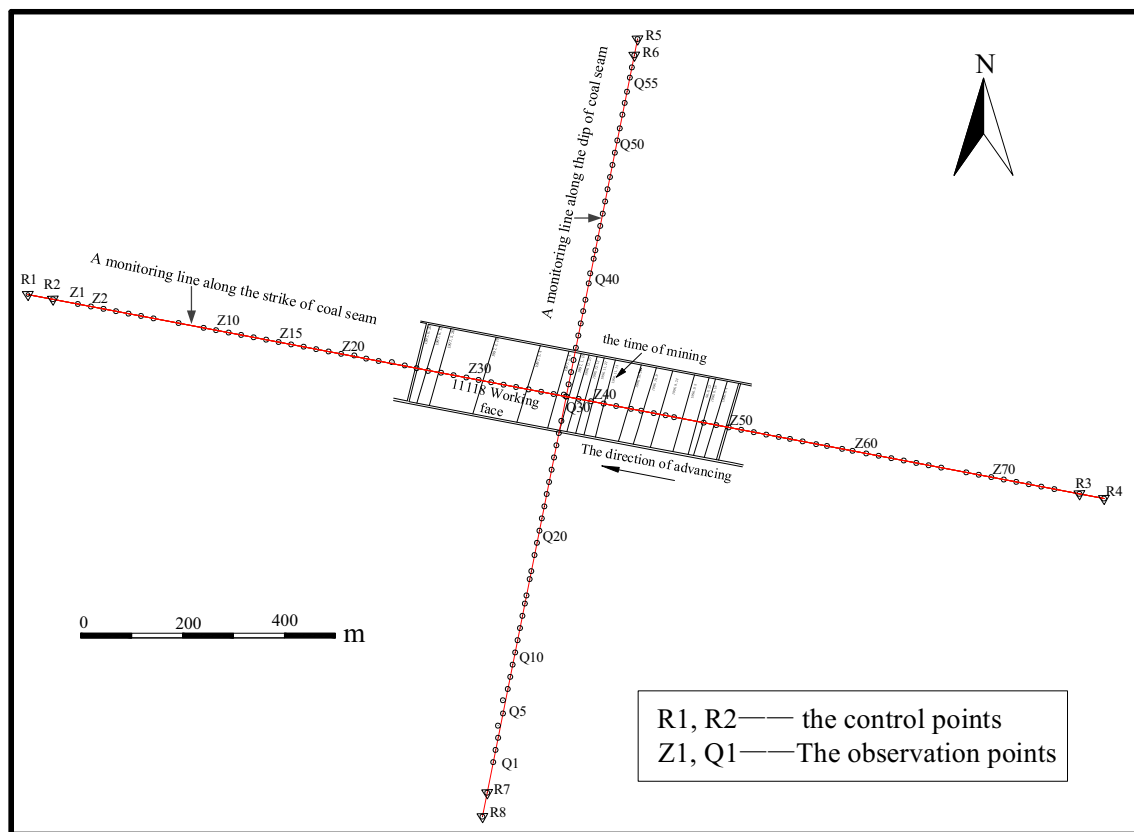


Fig. 4 Layout of the ground movement observation station on the working face A of the Xieqiao mine in the north area of the Huainan coal mining area

the Huainan coal mining area had a general similarity reaching 0.82.

From a stratigraphic perspective, both the Xieqiao and Xinzhuangzi mines belong to the same coalfield (see Fig. 3), namely the Huainan coal mining area, and their coal measurement strata are basically similar. Therefore, the overlying rock structure of the two coal mines is highly similar, and it is reasonable to take the ground subsidence measurement data (or field-measured parameters) of working face B2 in the Xinzhuangzi mine in the south area as the bedrock surface subsidence (or subsidence parameters) of working face A in the Xieqiao mine in the north area.

Table 2 shows that the bedrock height of the selected sample is 200 m, while the bedrock height of the standard sample is 150 m after removing the alluvial layer. While the subsidence profiles should be influenced by the height of the bedrock to a certain extent, in our special case, the selected sample is the best given the various factors, including the general similarity in the overlying rock structure, coal measurement strata, and same coalfield. Based on the premise that the lithology of the overlying rock and stratum structure is most similar—the general similarity in the overlying rock structure is the highest—

after a comprehensive comparison of various factors, we determined that the influence of differences in bedrock height on the subsidence profile was within an acceptable range. Bedrock with the same thickness is ideal, and we suggest to readers that consistent bedrock thickness be maintained in applying this method.

Finally, the Xinzhuangzi mine was selected as the N-CMATAS for study because its overlying rock structures were similar to those of the CMATAS of the Xieqiao mine. Using the proposed approach, therefore, we can take the measured ground subsidence (or the measured ground subsidence parameters) of the N-CMATAS of the Xinzhuangzi mine as the bedrock surface subsidence (or the bedrock surface subsidence parameters) of the CMATAS of the Xieqiao mine.

Determination of bedrock surface subsidence in the CMATAS of the Xieqiao mine

According to the theory of mining subsidence, based on the premise that the geo-mining conditions are the same or similar, when the overlying strata lithology and stratigraphic structure of two mining working faces are the same or similar, the ground subsidence parameters of the two

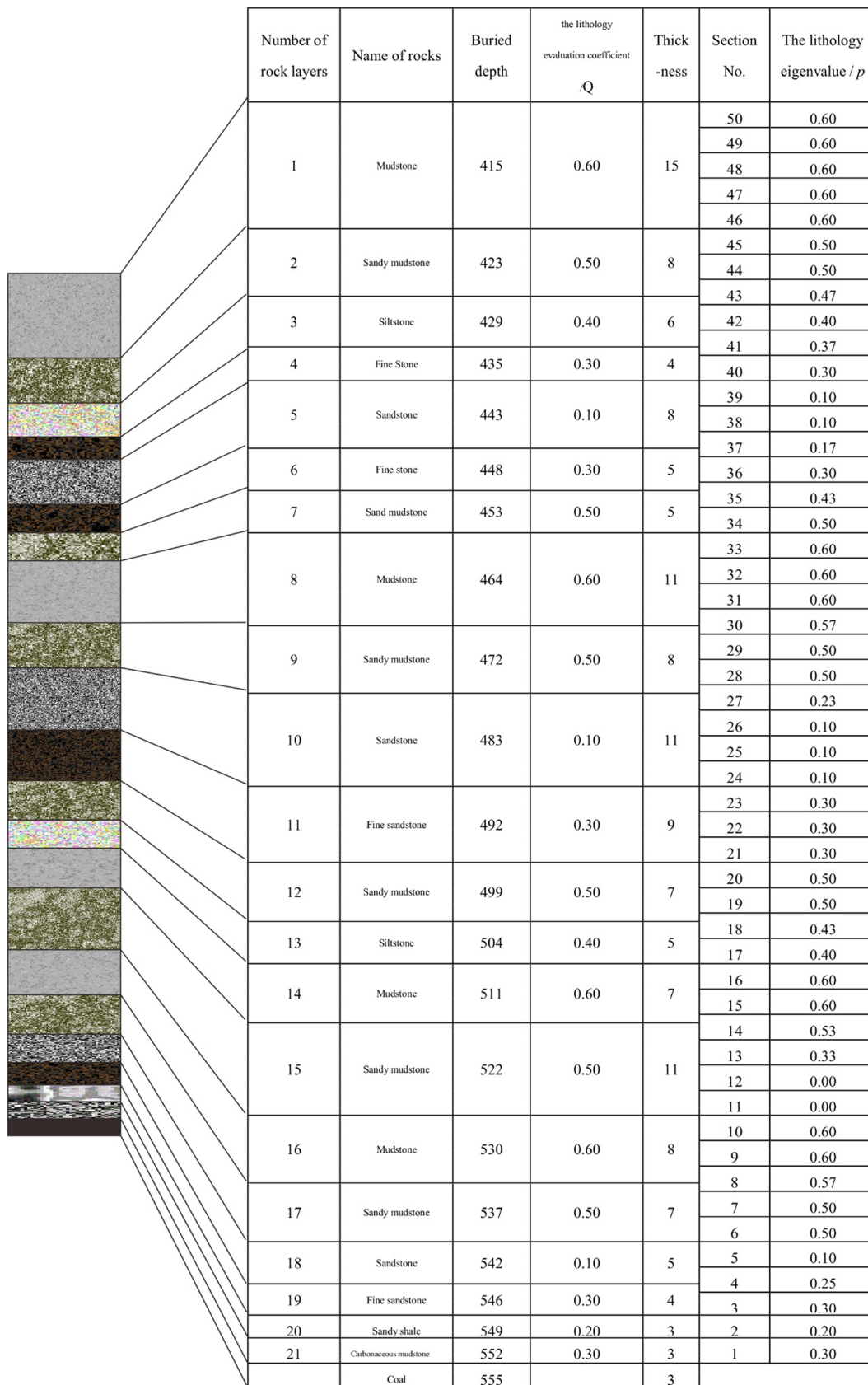


Fig. 5 The borehole log of working face A of the Xieqiao mine in the north area of the Huainan coal mining area

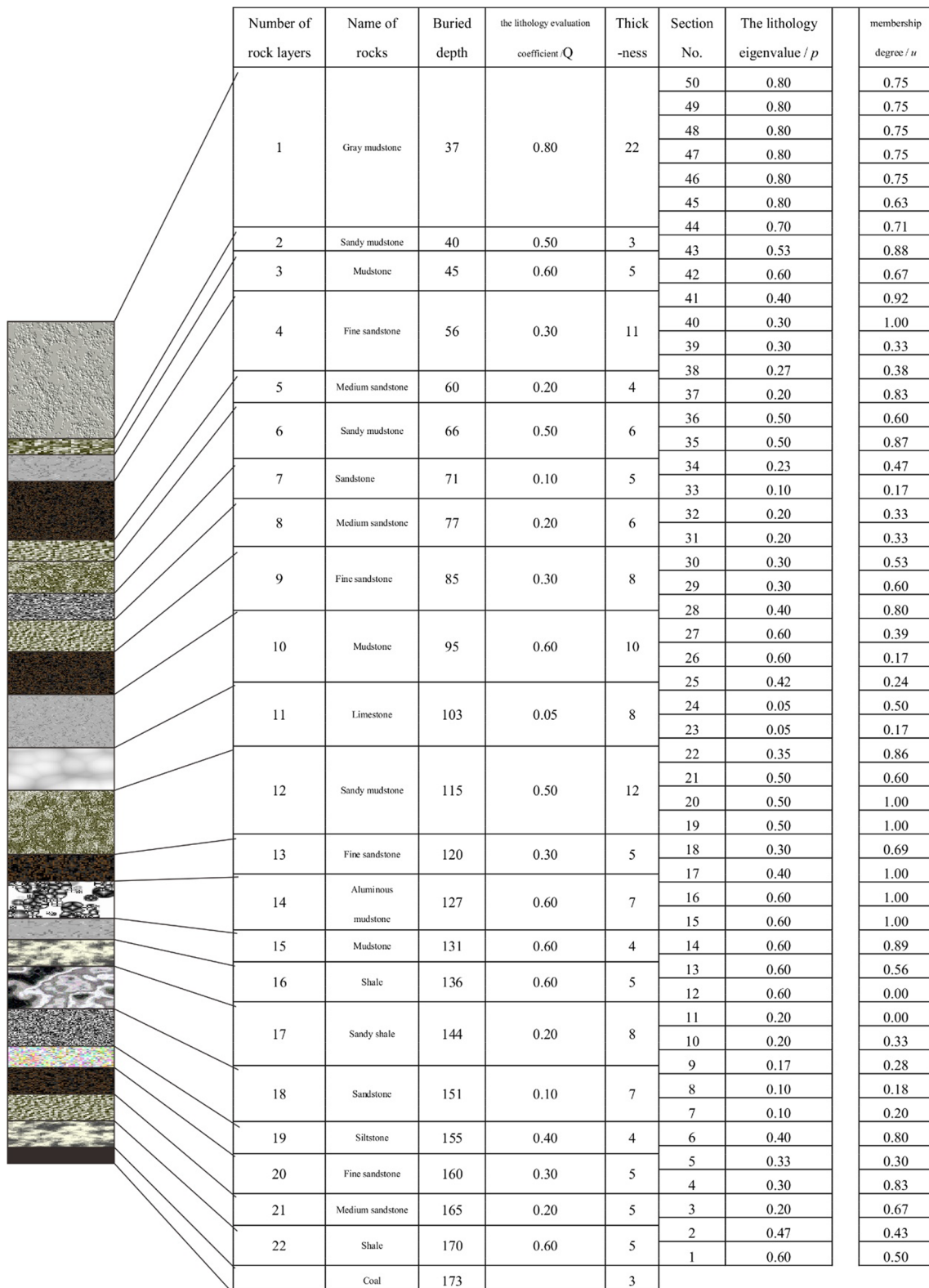


Fig. 6 The borehole log of working face B1 of the No. 4 mine of the Pingdingshan coal mining area

mining areas are also the same or similar. The size and number of ground observation points of working face B2 in the Xinzhuangzi mine and working face A in the Xieqiao

mine are different. Therefore, to make full use of the measured ground subsidence data of working face B2, we first obtained field-measured ground subsidence parameters

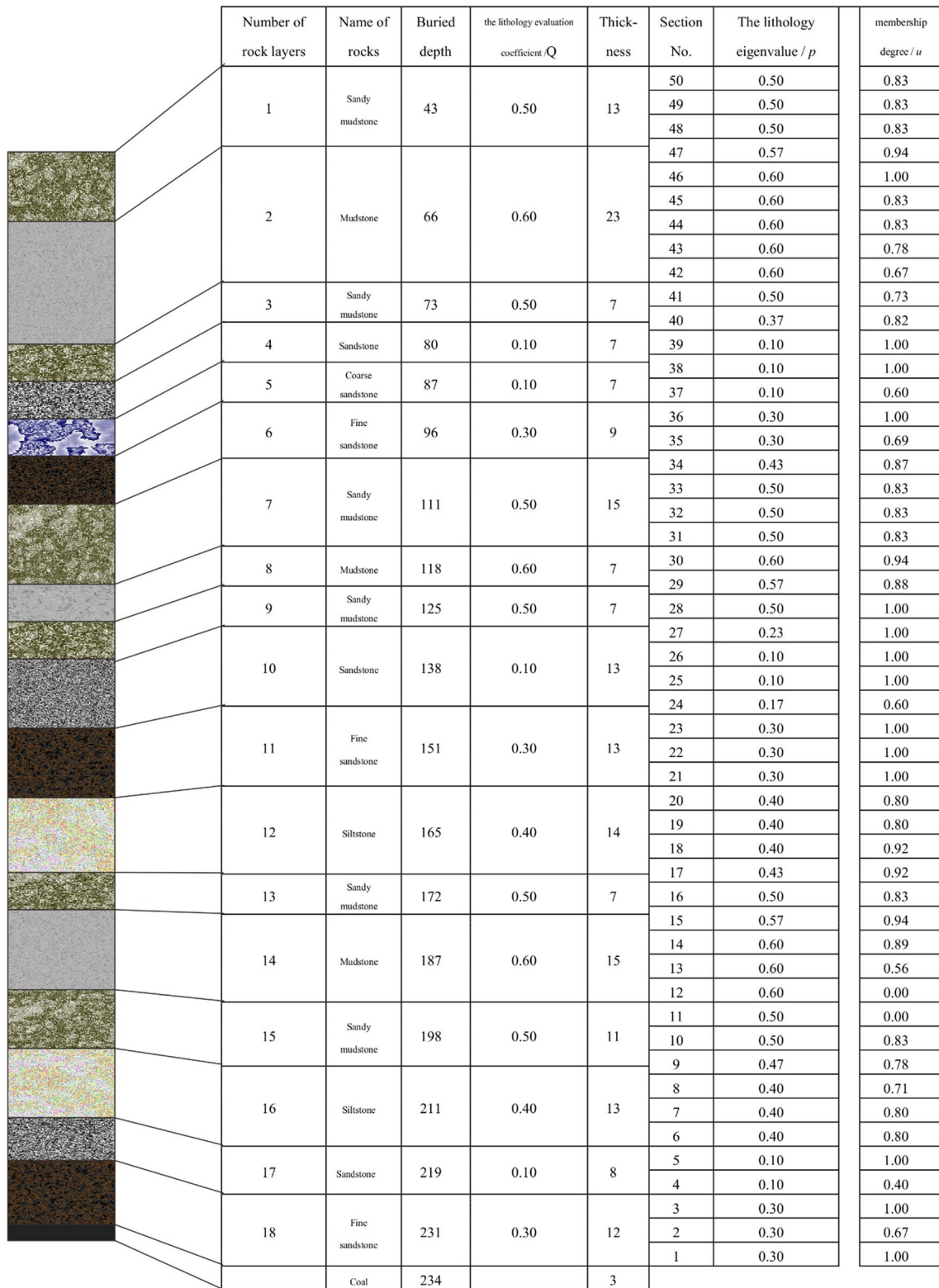


Fig. 7 The borehole log of working face B2 of the Xinzhuangzi mine in the south area of the Huainan coal mining area

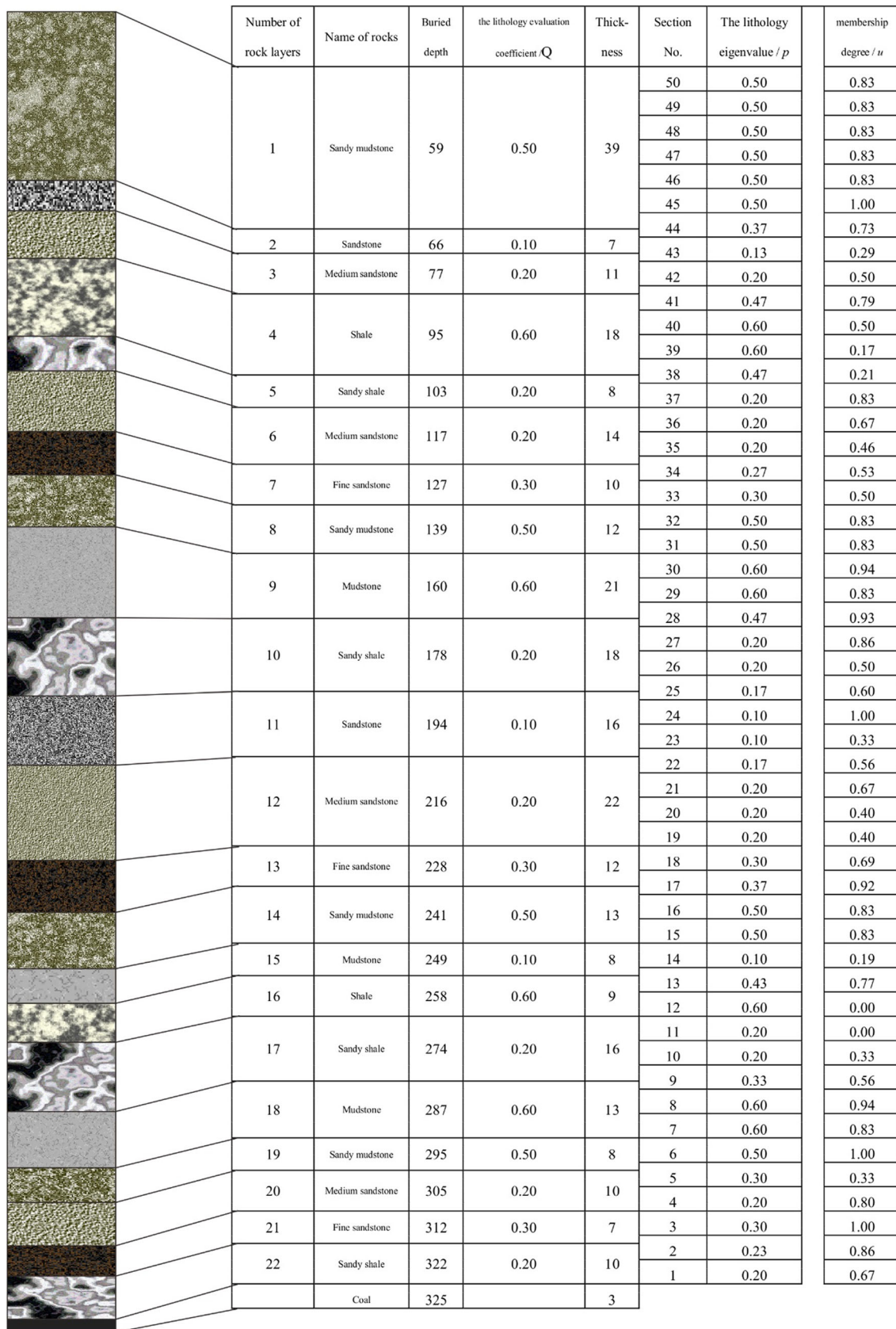


Fig. 8 The borehole log of working face B3 of the Yuanzhuang mine of the Huaibei coal mining area

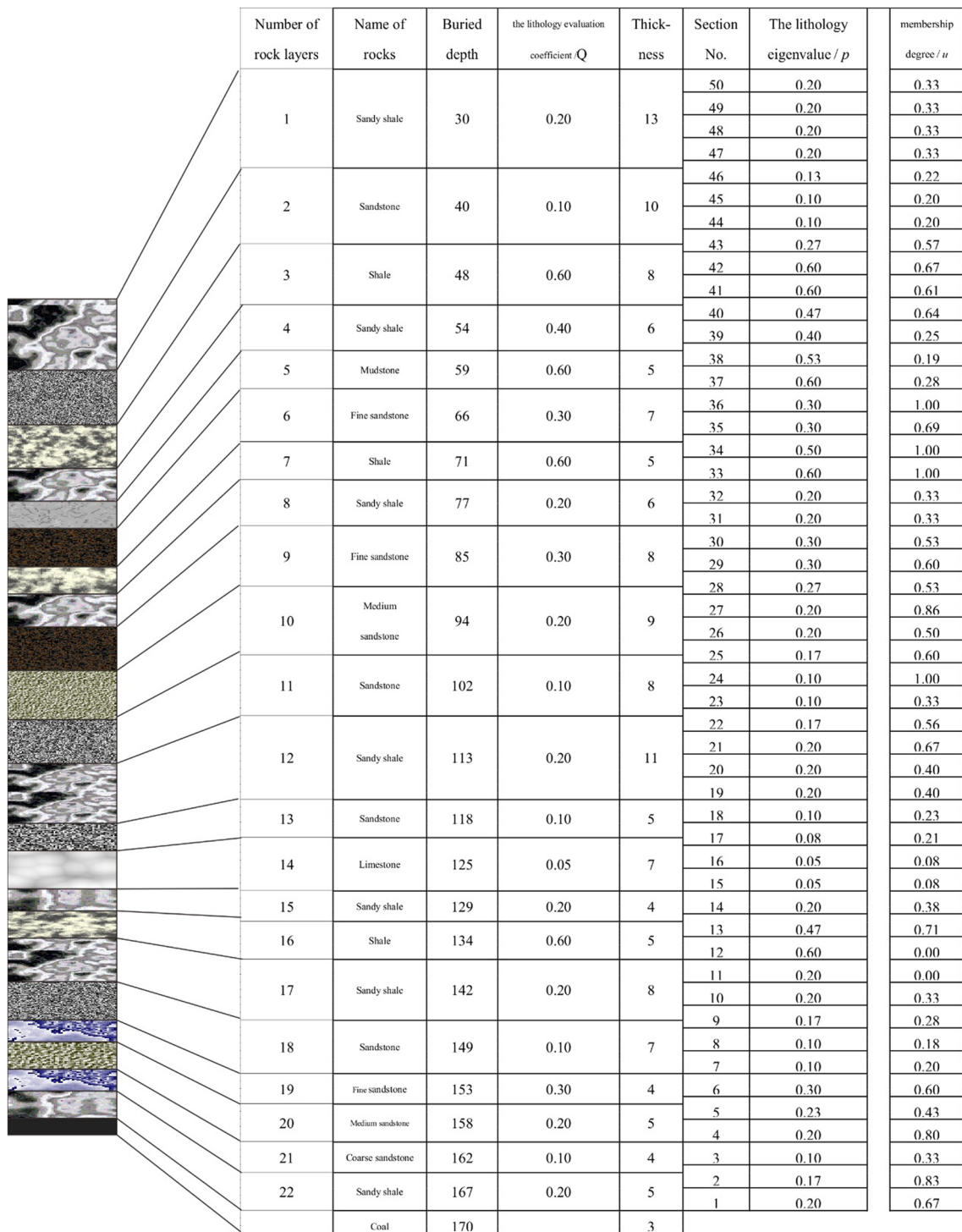


Fig. 9 The borehole log of working face B4 of the Quantai mine of the Xuzhou coal mining area

of the working face using the inversion of the probability integral method. The measured ground subsidence parameters of the N-CMATAS of the Xinzhuangzi mine were taken as the bedrock subsidence parameters of the CMA-TAS of the Xieqiao mine, and then on the basis of these

parameters, the bedrock subsidence of working face A of the Xieqiao mine was obtained using the probability integral method, which is an influence function method. In this manner, the lower boundary condition of the thick alluvium in the Xieqiao mine was determined.

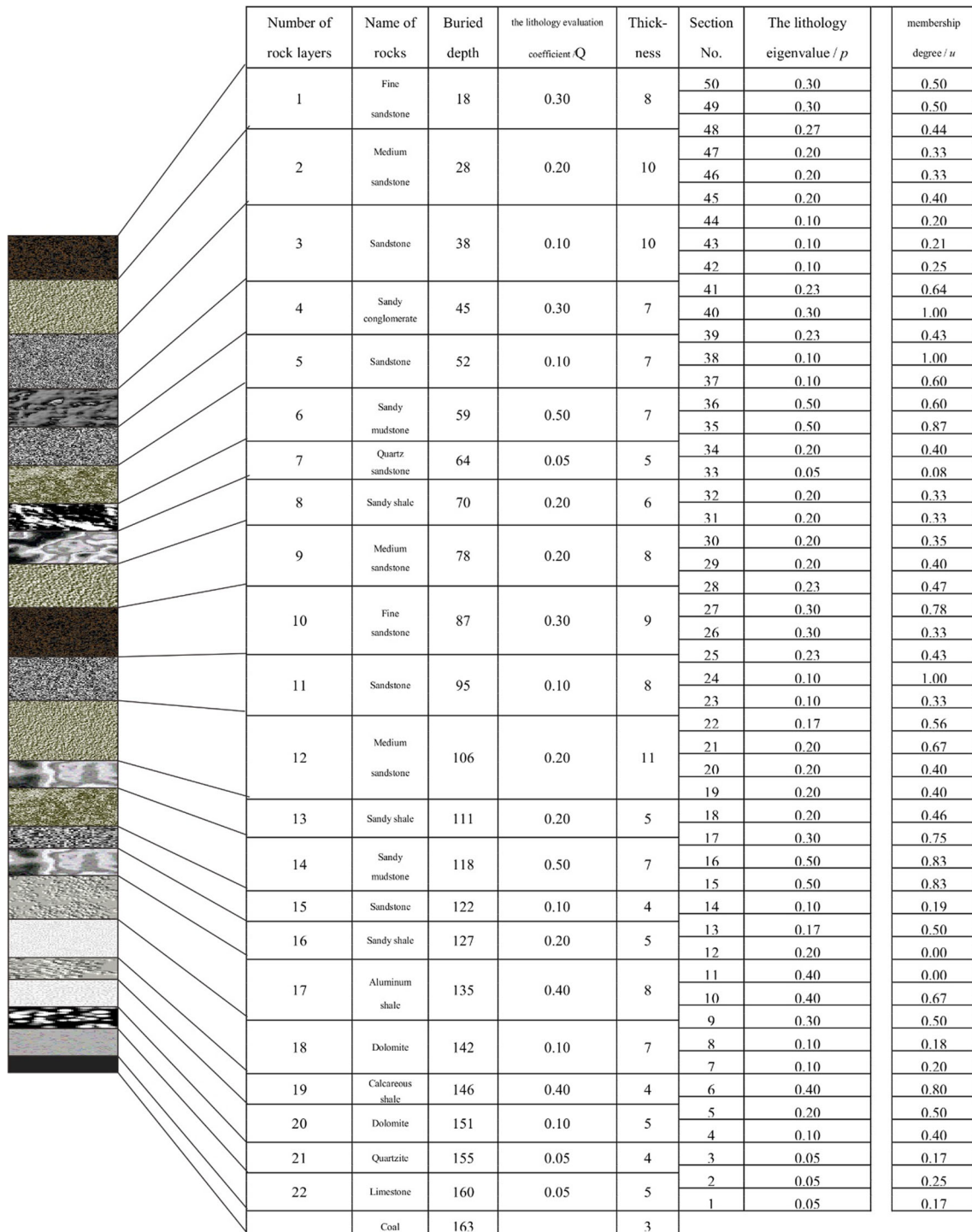


Fig. 10 The borehole log of working face B5 of the Fengfeng coal mining area

An influence function method and its inversion method

The probability integral method is a mining subsidence prediction model based on a flat-seam ore body (such as a coal seam), and overburden strata subsidence caused by unit mining is taken as a stochastic event in the model.

Event probability is represented by subsidence possibility and strata subsidence. The probability integral method model was named for its prediction formula containing the probability integral, and its basis is the theory of the random medium (Baochen and Ronggui 1981; Brady and Brown 2004; Cui et al. 2000, 2001; He et al. 1991;

Table 2 Geological and mining conditions in different mining areas

	Working face	Overlying rock structure	Geo-mining factors					Mining method	Method of roof control
			Coal seam thickness (m)	Dip angle (°)	Avg. mining depth (m)	Alluvial soil layer (m)			
Standard sample	Working face A of the Xieqiao mine in the north area of the Huainan coal mining area	Borehole log of Fig. 5	2.3	15	550	400	Longwall mining on the strike	Full caving	
Samples to be identified (working faces of thin (non-)alluvium)	Working face B1 of the No. 4 mine of the Pingdingshan coal mining area	Borehole log of Fig. 6	2.6	13	170	15	Longwall mining on the strike	Full caving	
	Working face B2 of the Xinzhuangzi mine in the south area of the Huainan coal mining area	Borehole log of Fig. 7	2.0	15	230	30	Longwall mining on the strike	Full caving	
	Working face B3 of the Yuanzhuang mine of the Huaibei coal mining area	Borehole log of Fig. 8	2.0	16	320	20	Longwall mining on the strike	Full caving	
	Working face B4 of the Quantai mine of the Xuzhou coal mining area	Borehole log of Fig. 9	2.1	20	160	17	Longwall mining on the strike	Full caving	
	Working face B5 of the Fengfeng coal mining area	Borehole log of Fig. 10	2.4	11	160	10	Longwall mining on the strike	Full caving	

Table 3 The general similarity between the samples to be identified and the standard sample

	Working face	Overlying rock structure	General similarity (C)
Standard sample	Working face A of the Xieqiao mine in the north area of the Huainan coal mining area	Borehole log of Fig. 5	
Samples to be identified [working faces of thin (non-)alluvium]	Working face B1 of the No. 4 mine of the Pingdingshan coal mining area	Borehole log of Fig. 6	0.59
	Working face B2 of the Xinzhuangzi mine in the south area of the Huainan coal mining area	Borehole log of Fig. 7	0.82
	Working face B3 of the Yuanzhuang mine of the Huaibei coal mining area	Borehole log of Fig. 8	0.68
	Working face B4 of the Quantai mine of the Xuzhou coal mining area	Borehole log of Fig. 9	0.46
	Working face B5 of the Fengfeng coal mining area	Borehole log of Fig. 10	0.46

Huayang et al. 2010; Industry SBoC 2004; Kratzsch 1983; Peng 1992). It has become the most widely used prediction method in China (He et al. 1991; Industry SBoC 2004).

The probability integral prediction model The probability integral model is used to illustrate the prediction model of an arbitrary point on the surface and to express the trough of surface subsidence caused by unit mining. It can be derived as follows:

$$W_e(x) = \frac{1}{r} e^{-\frac{x^2}{r^2}} \quad (4)$$

Considering the three-dimensional situation in Fig. 11, subsidence of arbitrary point A (x, y) on the surface caused by coal mining in unit B (s, t) is as follows:

$$W_e(x, y) = \frac{1}{r^2} e^{-\frac{(x-s)^2 + (y-t)^2}{r^2}} \quad (5)$$

When the mining area is O_1CDE as shown in Fig. 11, the prediction formula for subsidence of the arbitrary point (x, y) caused by the full mining process is as follows:

$$W(x, y) = W_0 \int_0^l \int_0^L \frac{1}{r^2} e^{-\frac{(x-s)^2 + (y-t)^2}{r^2}} dt ds, \quad (6)$$

$$V = \begin{pmatrix} V_1 \\ V_2 \\ \vdots \\ V_n \end{pmatrix}, Z = \begin{pmatrix} \Delta q \\ \Delta \tan \beta \\ \Delta S_1 \\ \Delta S_2 \\ \Delta S_3 \\ \Delta S_4 \\ \Delta \theta_0 \end{pmatrix}, L = \begin{pmatrix} l_1 \\ l_2 \\ \vdots \\ l_n \end{pmatrix}$$

although we know that the maximum subsidence W_0 in the influence function (Eq. 6) is fixed, in order to obtain the most realistic parameters, we still take subsidence q as a variable in the inversion calculation method. When the subsidence parameters ($q, \beta, S_1, S_2, S_3, S_4, \theta_0$) are viewed as variables, Eq. (6) can be expressed as Eq. (7) and further rewritten as Eq. (8).

$$B = \begin{pmatrix} \left(\frac{\partial f}{\partial q}\right)_1 & \left(\frac{\partial f}{\partial \tan \beta}\right)_1 & \left(\frac{\partial f}{\partial S_1}\right)_1 & \left(\frac{\partial f}{\partial S_2}\right)_1 & \left(\frac{\partial f}{\partial S_3}\right)_1 & \left(\frac{\partial f}{\partial S_4}\right)_1 & \left(\frac{\partial f}{\partial \theta_0}\right)_1 \\ \left(\frac{\partial f}{\partial q}\right)_2 & \left(\frac{\partial f}{\partial \tan \beta}\right)_2 & \left(\frac{\partial f}{\partial S_1}\right)_2 & \left(\frac{\partial f}{\partial S_2}\right)_2 & \left(\frac{\partial f}{\partial S_3}\right)_2 & \left(\frac{\partial f}{\partial S_4}\right)_2 & \left(\frac{\partial f}{\partial \theta_0}\right)_2 \\ \vdots & \vdots & \vdots & \vdots & \vdots & \vdots & \vdots \\ \left(\frac{\partial f}{\partial q}\right)_n & \left(\frac{\partial f}{\partial \tan \beta}\right)_n & \left(\frac{\partial f}{\partial S_1}\right)_n & \left(\frac{\partial f}{\partial S_2}\right)_n & \left(\frac{\partial f}{\partial S_3}\right)_n & \left(\frac{\partial f}{\partial S_4}\right)_n & \left(\frac{\partial f}{\partial \theta_0}\right)_n \end{pmatrix}$$

Using the principle of least squares, i.e., $V^T V = \min$, we can obtain the normal equation:

$$B^T B Z + B^T L = 0 \tag{11}$$

Solving Eq. (11), parameter correction can be achieved; by adding the correction to the initial approximation parameters, we can obtain accurate parameters.

The maximum subsidence W_0 is fixed for a mine. Based on the function $W_0 = mq \cos \alpha$, we can obtain the subsidence factor q . In this study, however, we did not use the maximum subsidence to obtain the subsidence factor q , for two main reasons. First, the maximum subsidence appears only by extending the range of extraction to the critical area, and the subsidence factor q can be obtained using the maximum subsidence. At present, it is difficult for the size of a working face to reach the critical area. Second, if we use only maximum subsidence W_0 to obtain the subsidence factor q , the fit is good at the location of the maximum subsidence and poor in other areas. A good overall fit is vital in mining subsidence theory, so the subsidence factor q is taken as a variable. Through the circle variation of subsidence factor q and other parameters such as those in Eq. (7), we can use the principle of least squares to fit the predicted subsidence of the monitored sample and obtain more realistic subsidence parameters, including subsidence factor q . Therefore,

Using the aforementioned inversion calculation method, we obtained the ground subsidence parameters of working face B2 of the Xinzhuangzi mine (Table 4). The calculated subsidence parameters are also considered as the bedrock surface subsidence parameters of the CMATAS of the Xieqiao mine.

Calculation results

Based on the field-measured subsidence parameters of working face B2 (Table 4) and Eq. (6), the bedrock surface subsidence of working face A can be predicted using the probability integral prediction model. The bedrock surface subsidence profile of the CMATAS of the Xieqiao mine is shown in curves (2) of Figs. 12 and 13, which are taken as the lower boundary conditions of the thick alluvium.

The field-measured ground subsidence of working face A (Fig. 4 is the GMOS, and we use levelling to monitor the ground subsidence of observation points) is shown in curves (1) of Figs. 12 and 13, which is taken as the upper boundary conditions of the thick alluvium.

We have determined the geological and mining conditions of the CMATAS of the Xieqiao mine during underground mining and obtained the upper and lower boundary conditions of the thick alluvium in the Xieqiao mine.

Table 4 Field-measured ground subsidence parameters of the Xinzhuangzi mine in the south area

Subsidence factor (q)	Tangent of main effect angle ($\tan \beta$)	Effect transference angle, θ_0 ($^\circ$)	Left deviation of inflection point S_1 (m)	Right deviation of inflection point S_2 (m)	Raise deviation of inflection point S_3 (m)	Dip deviation of inflection point S_4 (m)
0.81	1.9	82	10	-4	8	-6

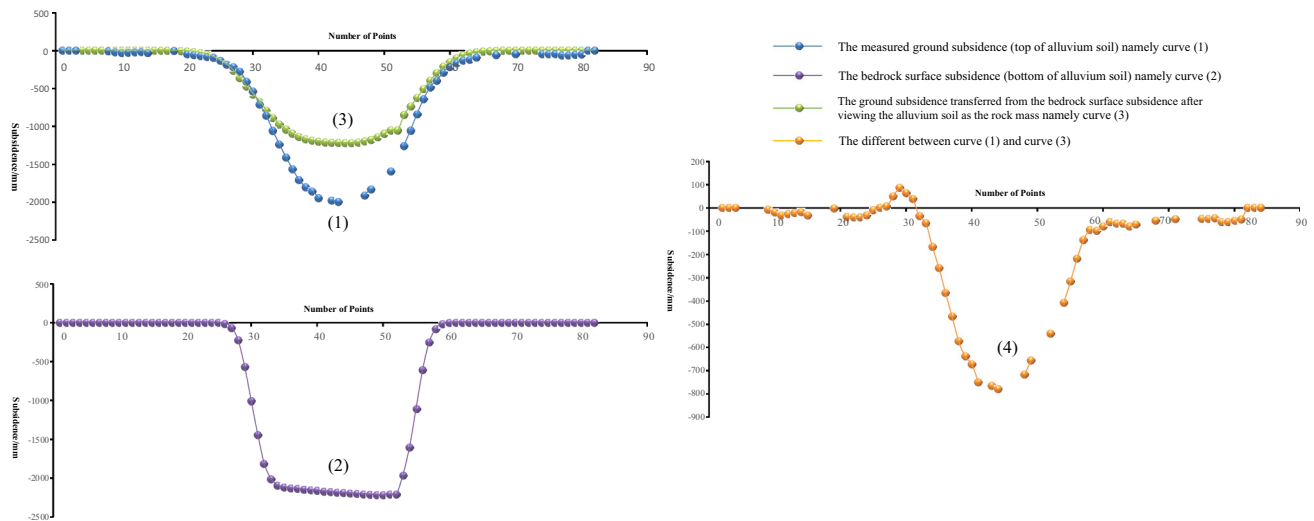


Fig. 12 Subsidence of working surface A in the Xieqiao mine in the north area along the strike direction

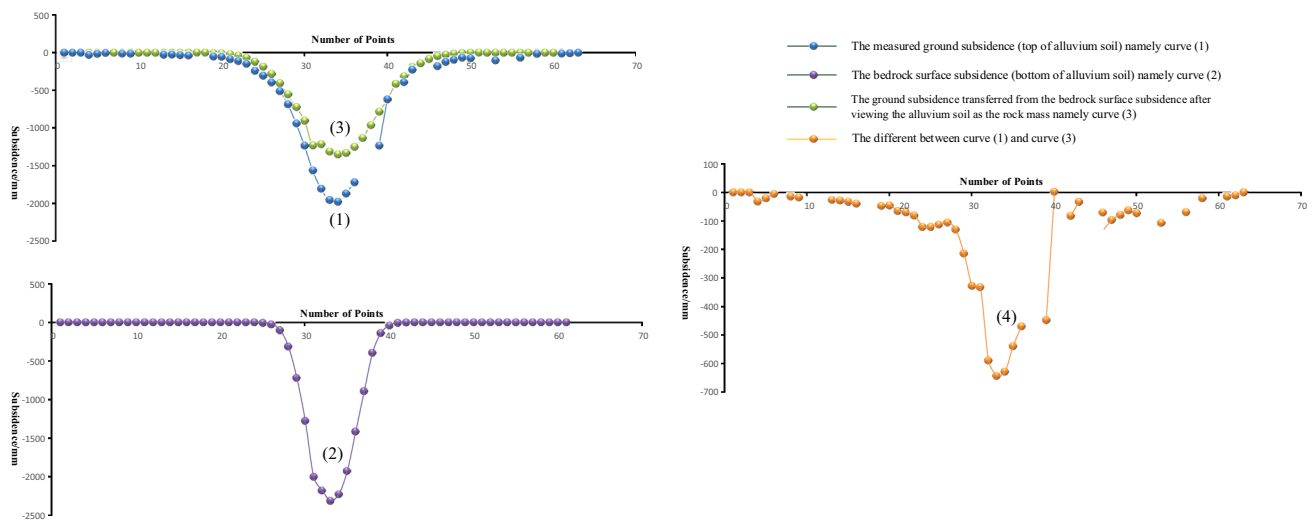


Fig. 13 Subsidence of working surface A in the Xieqiao mine in the north area along the dip direction

Consequently, we can carry out analysis of the spreading process of mining subsidence in the rock mass and alluvial soil.

Spreading of mining subsidence in rock mass and alluvial soil

Spreading inside rock mass

As shown in curves (2) of Figs. 12 and 13, the underground mining space (goaf) is shaped after coal is mined out; when the space/goaf is large enough, the overlying strata is damaged, and caving, fracture, and bend zones form in the strata from the bottom to the top. Meanwhile, the underground space is transferred up through the rock mass, and

the subsidence trough is first formed on the bedrock surface. The curves (2) illustrate bedrock subsidence profiles along the strike and dip directions.

According to the data obtained, the thickness of the coal seam is about 3.0 m after mining; however, from curves (2), the maximum subsidence of the bedrock surface is about 2.3 m (2300 mm). In other words, during the spreading process of mining subsidence inside the rock mass, subsidence weakens. After the bedrock over the coal mining panel is broken, the broken rock mass will expand and the rock fracture will increase (Brady and Brown 2004; Hao 1988; He et al. 1991; Peng 1992). In this way, the extraction space underground is fixed; when the gap (space) contained inside the rock mass increases, the bedrock surface subsidence should decrease. Therefore, the

expansion of broken rocks and increasing gaps (space) inside broken rocks are responsible for the weakening of the bedrock surface subsidence.

Spreading inside alluvial soil

The thickness of alluvium in the Xieqiao mine is about 400 m. The bedrock surface subsidence space (i.e., the bedrock surface subsidence trough) spreads continually to the alluvial mass, and eventually a ground subsidence trough is formed. Based on the field-measured ground subsidence of the Xieqiao mine (GMOS in Fig. 4), the ground subsidence profiles along the strike and dip directions are shown in the curves (1) of Figs. 12 and 13. The maximum ground subsidence is about 2.0 m (2000 mm).

If alluvium of 400-m thickness is taken as rock mass, the degree of ground subsidence when the bedrock surface subsidence spreads to the ground through the rock mass is unknown. However, we can calculate the subsidence using the influence function, i.e., the probability integral prediction method:

- The primary premise and hypothesis of the probability integral prediction method is based on the sandbox model, which considers large areas of broken rock mass from underground coal mining as sand; therefore, rock mass subsidence behaves in a manner similar to the hourglass model. According to current data (Baochen and Ronggui 1981; Brady and Brown 2004; Hao 1988; Hao and Ma 1985, 1986; He 1982; He et al. 1991; Industry SBoC 2004; Kratzsch 1983; Liu 1981; Sui 1992; Wu et al. 2013; Yuan and Wu 2003; Zhang et al. 1999), the probability integral prediction method is suitable for the N-CMATASs, and the overall accuracy of the calculation is quite high. Based on the features of the influence function, we can obtain the ground subsidence after the 400-m alluvium is taken as rock mass.
- According to the field-measured subsidence parameters of working face B2 (see Table 4), we calculate subsidence up to the ground surface—coal mining depth increased by 400 m from the coal mining face to the bedrock surface—using the probability integral prediction model to obtain the ground subsidence transferred from the bedrock surface subsidence of the Xieqiao mine. The final calculated ground subsidence profiles are shown in curves (3) of Figs. 12 and 13 (taking alluvium as rock mass). From curves (3), the calculated maximum ground subsidence is about 1.22 m (1220 mm).

From curves (1) and (3) in Figs. 12 and 13, we can see that the ground subsidence value transferred from the bedrock surface subsidence through the thick alluvial mass

is greater than that transferred from the bedrock surface subsidence through the rock mass. The maximum difference in the ground subsidence formed while spreading between the thick alluvium and the rock mass reaches 780 mm. Curve (4) shows the difference between curve (1) and corresponding curve (3). Alluvium exhibits compression and consolidation characteristics, while rock mass features broken expansions. The different properties of the alluvium and rock mass cause differences in ground subsidence.

The thick alluvium is disturbed during the progression of bedrock surface subsidence spreading through the alluvium to the ground surface, and the disturbance can alter the internal structure of the alluvium, resulting in additional stress. For example, pore water inside the alluvium is extruded and pore pressure in the disturbed location increases, adding stress inside the alluvium (Brady and Brown 2004; He et al. 1991; Huayang et al. 2010; Industry SBoC 2004; Kratzsch 1983; Peng 1992; Zhou 2014; Zhou et al. 2015). Under this additional stress, the thick alluvium experiences compression deformation, which causes additional subsidence inside the alluvium. This additional subsidence would increase the ground subsidence in the CMATAS in the Xieqiao mine. This is the first reason that the ground subsidence in a CMATAS is greater than that in an N-CMATAS.

The influence of the thick alluvium on the goaf in the form of load results in compact fractured rock mass, and more closed separated layers are formed, thus inhibiting developments in the height of the fractured water-conducting zone. The rock gap (space) displaced is transferred to the bedrock surface in the form of subsidence, which increases the subsidence of the bedrock surface and further increases the ground surface subsidence. Such subsidence caused by the influence of thick alluvium on the goaf is referred to as synergy subsidence between the thick alluvium and goaf. This is the second reason for the greater surface subsidence in a CMATAS than in an N-CMATAS.

The additional subsidence inside the thick alluvium and the synergy subsidence between the thick alluvium and goaf are together defined as the response of soil to mining subsidence, which is different from mining subsidence under conventional geological conditions (N-CMATASs). Therefore, it is clear that the field-measured ground subsidence [curves (1) of Figs. 12 and 13] includes the response of soil to mining subsidence, which explains why mining subsidence in coal mining areas with thick alluvium is so complex.

According to the analysis above, curves (1) of Figs. 12 and 13 is the field-measured ground subsidence curve, which is a composite subsidence curve integrating the response of the soil to mining subsidence. Therefore, curves (4) of Figs. 12 and 13 acquired by curves (3)

subtracted from curves (1) reflect all additional subsidence of the alluvial mass—the response of the soil to mining subsidence. Curves (4) of Figs. 12 and 13 show that the maximum additional subsidence of working face A in the Xieqiao mine amounts to 780 mm (the total amount of the response of the soil to mining subsidence).

What is the extent of vertical subsidence induced by thick alluvium? In other words, to what degree does the response of thick alluvium to mining subsidence account for of the total ground subsidence? It is difficult to answer this question using existing methods. In this study, therefore, we put forward a new approach to solving the problem. Using this approach, we can determine the response of soil to mining subsidence. This novel method can be universally applied, supports new ideas and technical approaches for researchers in the field, provides measured data for research on mining subsidence in areas covered with thick alluvium, and promotes more comprehensive development of the subject. The proposed method was successfully applied in the Huainan coal mining area in China (3).

Conclusions

In this work, we have analyzed the unique features and the results of the present research on ground subsidence in CMATASs. In addition, we have identified the shortcomings of current research methods, which mainly involve numerical/physical simulation and theoretical analysis, and lack convincing verification in the form of field-measured data, which limits the applicability of the research results and leads to weak practicability.

In this study, from the perspective of fully utilizing field-measured data, we have proposed a new approach to compensate for the shortfalls and to study the response of soil to mining subsidence in CMATASs, and we have presented an overview of the research and methodology of the approach. A prominent feature of the proposed approach is that the overlying rock mass and alluvium are regarded as a dual medium, and can be separated through the measured data of the upper and lower boundaries of the thick alluvium, which compensates for the shortage of measured data in current study methods. The proposed method was successfully applied in the Huainan coal mining area in China.

The method proposed in this study, with its universal applicability, provides a new conceptual and technical approach for researchers in the field. In addition, it can provide measured data for research of mining subsidence in areas covered with thick alluvium, promoting a more comprehensive development of the subject.

Acknowledgments This research was financially supported by the Natural Science Foundation of Jiangsu Province (BK20150187), the Priority Academic Program Development of the Jiangsu Higher Education Institutions (PAPD), the National Technology Support Programs of China during the Twelfth Five-Year Plan Period (2012BAC04B03), and the National Natural Science Foundation of China (51504239). The authors gratefully acknowledged all of this financial supports. We are especially grateful to the reviewers for their helpful comments, which improved the paper.

References

- Alejano LR, Ramirez-Oyanguren P, Taboada J (1999) FDM predictive methodology for subsidence due to flat and inclined coal seam mining. *Int J Rock Mech Min Sci* 36:475–491. doi:10.1016/S0148-9062(99)00022-4
- Baochen L, Ronggui Y (1981) The basic rules of displacement of rock mass due to underground mining. *J China Coal Soc* 1:40–55
- Brady BHG, Brown ET (2004) *ROCK mechanics for underground mining*, 3rd edn. Springer, London
- Caro Cuenca M, Hooper AJ, Hanssen RF (2013) Surface deformation induced by water influx in the abandoned coal mines in Limburg, The Netherlands observed by satellite radar interferometry. *J Appl Geophys* 88:1–11. doi:10.1016/j.jappgeo.2012.10.003
- Chai J, Shen S, Zhu H, Zhang X (2004) Land subsidence due to groundwater drawdown in Shanghai. *Geotechnique* 54:1143–1147
- Cui XM et al (2000) Improved prediction of differential subsidence caused by underground mining. *Int J Rock Mech Min Sci* 37:615–627. doi:10.1016/S1365-1609(99)00125-2
- Cui X, Wang JC, Liu Y (2001) Prediction of progressive surface subsidence above longwall coal mining using a time function. *Int J Rock Mech Min Sci* 38:1057–1063
- Cundall PA (1990) Numerical modeling of jointed and faulted rock. Paper presented at the international conference on mechanics of jointed and faulted rock, Vienna, Austria
- Djamaluddin I, Mitani Y, Esaki T (2011) Evaluation of ground movement and damage to structures from Chinese coal mining using a new GIS coupling model. *Int J Rock Mech Min Sci* 48:380–393. doi:10.1016/j.ijrmms.2011.01.004
- Donnelly LJ, De La Cruz H, Asmar I, Zapata O, Perez JD (2001) The monitoring and prediction of mining subsidence in the Amaga, Angelopolis, Venecia and Bolombolo Regions, Antioquia, Colombia. *Eng Geol* 59:103–114. doi:10.1016/S0013-7952(00)00068-5
- Gao M, Yu Z (2007) Repetitive mining subsidence with thick soil layers and steep seam. *J China Coal Soc* 32:347–352
- Ge X, Yu G (2006) Influence of underground mining on ground surface and railway bridge under thick alluvium. *J China Univ Min Technol* 16:97–100
- Guéguen Y et al (2009) Monitoring residual mining subsidence of Nord/Pas-de-Calais coal basin from differential and persistent scatterer interferometry (Northern France). *J Appl Geophys* 69:24–34. doi:10.1016/j.jappgeo.2009.02.008
- Hao Q (1988) Void diffusion model for mined strata and analysis of influence of void sources. *J China Univ Min Technol* 2:30–36
- Hao Q, Ma W (1985) On the methods of ground subsidence prediction. *J China Univ Min Technol* 2:37–42
- Hao Q, Ma W (1986) The optimum form of Weibull distribution subsidence equation and its application in surface subsidence calculation. *J China Univ Min Technol* 3:32–42
- He G (1982) Application of influence function of Weber distribution to the precalculation of ground surface movement: a study on the fundamental law of ground movement based on the clastic theory. *J China Univ Min Technol* 1:1–20

- He G, Yang L, Ling G, Jia C, Hong D (1991) Mining subsidence science. China University of Mining and Technology Press, Xuzhou
- Holla L (1997) Ground movement due to longwall mining in high relief areas in New South Wales, Australia. *Int J Rock Mech Min Sci* 34:775–787
- Huayang D, Xugang L, Jiyang L, Yixin L, Yameng Z, Weinan D, Yinfei C (2010) Model study of deformation induced by fully mechanized caving below a thick loess layer. *Int J Rock Mech Min Sci* 47:1027–1033. doi:10.1016/j.ijrmms.2010.06.005
- Industry SBoC (2004) The regulation of leaving coal pillar and mining coal of holding under the buildings, water bodies, railways and the main roadway. Coal Industry Press, Beijing
- Kidybinski A, Babcock CO (1973) Stress distribution and rock fracture zones in the roof of Longwall face in a coal mine. *Rock Mech* 5:1–19
- Kratzsch H (1983) Mining subsidence engineering. Springer, Berlin
- Li W, Yu S (1997) Engineering geological characteristics and mechanism of deformation due to water loss of the soil mass at depths in Xuhuai mine area. *J China Coal Soc* 22:355–360
- Li W-X, Wen L, Liu X-M (2010) Ground movements caused by deep underground mining in Guan-Zhuang iron mine, Luzhong, China. *Int J Appl Earth Obs Geoinform* 12:175–182. doi:10.1016/j.jag.2010.02.005
- Li L, Wu K, Zhou DW (2014) AutoCAD-based prediction of 3D dynamic ground movement for underground coal mining. *Int J Rock Mech Min Sci* 71:194–203. doi:10.1016/j.ijrmms.2014.04.025
- Liu Y (1981) Surface movements, overburden failure and its application. Coal Industry Press, Beijing
- Liu Y, Dai H, Jiang Y (2012) Model test for mining-induced movement law of rock and soil mass under thick unconsolidated layers. *J Min Saf Eng* 29:268–272
- Lu Y, Wang L (2015) Numerical simulation of mining-induced fracture evolution and water flow in coal seam floor above a confined aquifer. *Comput Geotechnol* 67:157–171. doi:10.1016/j.compgeo.2015.03.007
- Marschalko M, Bednárík M, Yilmaz I, Bouchal T, Kubečka K (2011) Evaluation of subsidence due to underground coal mining: an example from the Czech Republic. *Bull Eng Geol Environ* 71:105–111. doi:10.1007/s10064-011-0401-8
- Nicieza CG, Fernandez MIA, Diaz AM, Vigil AEA (2005) The new three-dimensional subsidence influence function denoted by n-k-g. *Int J Rock Mech Min Sci* 42:372–387. doi:10.1016/j.ijrmms.2004.12.003
- Oconnor KM, Dowding CH (1992) Distinct element modeling and analysis of mining-induced subsidence. *Rock Mech Rock Eng* 25:1–24. doi:10.1007/Bf01041873
- Ortega-Guerrero A, Rudolph DL, Cherry JA (1999) Analysis of long-term land subsidence near Mexico City: field investigations and predictive modeling. *Water Resour Res* 35:3327–3341. doi:10.1029/1999wr900148
- Peng SS (1992) Surface subsidence engineering. Littleton Society for Mining, Metallurgy, New York
- Peng S, Zhang J (2007) Engineering geology for underground rocks. Springer, Berlin
- Phien-vej N, Giao PH, Nutalaya P (2006) Land subsidence in Bangkok. *Thail Eng Geol* 82:187–201. doi:10.1016/j.enggeo.2005.10.004
- Qian M, Miao X, Xu J, Mao X (2003) Study of key strata theory in ground control. China University of Mining and Technology Press, Xuzhou
- Ren W, Guo C, Peng Z, Wang Y (2010) Model experimental research on deformation and subsidence characteristics of ground and wall rock due to mining under thick overlying terrane. *Int J Rock Mech Min Sci* 47:614–624. doi:10.1016/j.ijrmms.2009.12.012
- Ronning JS, Lauritsen T, Mauring E (1995) Locating bedrock fractures beneath alluvium using various geophysical methods. *J Appl Geophys* 34(151):158. doi:10.1016/0926-9851(96)80894-9
- Sheorey PR, Loui JP, Singh KB, Singh SK (2000) Ground subsidence observations and a modified influence function method for complete subsidence prediction. *Int J Rock Mech Min Sci* 37:801–818. doi:10.1016/S1365-1609(00)00023-X
- Singh RP, Yadav RN (1995) Prediction of subsidence due to coal mining in Raniganj coalfield, West Bengal, India. *Eng Geol* 39:103–111
- Sui W (1992) Mechanism and prediction of soil mass deformation due to mining subsidence. Dissertation, China University of Mining and Technology
- Sui W, Di Q (1999) Study on interaction between soil mass deformation and pore pressure during subsidence by mining. *J Eng Geol* 07:303–307
- Tan Z, Deng K, Yang J (2002) Research on ground movement laws for strip mining under thick alluvium. *J China Univ Min Technol* 12:61–64
- Wang J, Li Y, Zhou X, Wu L, Wei S (1997) Ground movement caused by mining under thick alluvium. *J China Coal Soc* 22:18–21
- Wu K, Ge J, Wang LD, Zhou M (1998) Unify method of mining subsidence prediction. China University of Mining and Technology Press, Xuzhou
- Wu K, Deng K, Zhou M, Huang Z, Zheng Y, Wang Z (1999) The analysis of monitor conclusion about overburden displacement under condition of fully mechanized sublevel caving. *J China Coal Soc* 24:21–24
- Wu K, Wang Y, Deng K (2000) Application for dynamic mechanics model of overlying strata movement and damage above goaf. *J China Univ Min Technol* 29:34–36
- Wu K, Jin J, Dai Z, Jiang J (2002) The experimental study on the transmit of the mining subsidence in soil. *J China Coal Soc* 27:601–603
- Wu Q, Fan S, Zhou W, Liu S (2013) Application of the analytic hierarchy process to assessment of water Inrush: a case study for the No. 17 Coal Seam in the Sanhejian Coal Mine. *China Mine Water Environ* 32:229–238. doi:10.1007/s10230-013-0228-6
- Wu K, Cheng G-L, Zhou D-W (2014) Experimental research on dynamic movement in strata overlying coal mines using similar material modeling. *Arab J Geosci* 8:6521–6534. doi:10.1007/s12517-014-1685-3
- Xu Y-S, Shen S-L, Cai Z-Y, Zhou G-Y (2007) The state of land subsidence and prediction approaches due to groundwater withdrawal in China. *Nat Hazards* 45:123–135. doi:10.1007/s11069-007-9168-4
- Xue Y-Q, Zhang Y, Ye S-J, Wu J-C, Li Q-F (2005) Land subsidence in China. *Environ Geol* 48:713–720. doi:10.1007/s00254-005-0010-6
- Yang ZZ, Wang JC, Lu FW (1994) Technical counter measures for coal mining under buildings, water-bodies and railways in Huainan coal mines. *J China Coal Soc* 19:5–14
- Yasitli NE, Unver B (2005) 3D numerical modeling of longwall mining with top-coal caving. *Int J Rock Mech Min Sci* 42:219–235. doi:10.1016/j.ijrmms.2004.08.007
- Yuan L, Wu K (2003) Theoretical research and technology practice on mining under the Huaihe River embankment. China University of mining and technology press, Xuzhou
- Yuan L, Wu K, Du G, Tan Z (2001) monitoring of Huaihe Dike deformation caused by mining. *J China Univ Min Technol* 11:14–19
- Zhang X, Zhao Y, Liu S (1999) A new method of calculating surface subsidence and deformations under thick alluvial soil the Chinese. *J Nonfer Metals* 09:435–440
- Zhang WY, Wang WG, Peng WD, Feng ZH, Shun KS (2002) The coal mining practice of reducing waterproof coal pillars in Panxie mining area. *J China Coal Soc* 27:128–133

- Zhao H, Ma F, Xu J, Guo J (2012a) In situ stress field inversion and its application in mining-induced rock mass movement. *Int J Rock Mech Min Sci* 53:120–128. doi:[10.1016/j.ijrmms.2012.05.005](https://doi.org/10.1016/j.ijrmms.2012.05.005)
- Zhao H, Ma F, Zhang Y, Guo J (2012b) Monitoring and analysis of the mining-induced ground movement in the Longshou Mine, China. *Rock Mech Rock Eng* 46:207–211. doi:[10.1007/s00603-012-0232-3](https://doi.org/10.1007/s00603-012-0232-3)
- Zhou DW (2014) The synergy mechanism between rock mass and soil in mining subsidence and its prediction. Dissertation, China University of Mining and Technology
- Zhou D, Wu K, Chen R, Li L (2013) GPS/terrestrial 3D laser scanner combined monitoring technology for coal mining subsidence: a case study of a coal mining area in Hebei, China. *Nat Hazards* 70:1197–1208. doi:[10.1007/s11069-013-0868-7](https://doi.org/10.1007/s11069-013-0868-7)
- Zhou DW, Wu K, Cheng GL, Li L (2015) Mechanism of mining subsidence in coal mining area with thick alluvium soil in China. *Arab J Geosci* 8:1855–1867. doi:[10.1007/s12517-014-1382-2](https://doi.org/10.1007/s12517-014-1382-2)